

Circ_0020123 plays an oncogenic role in non-small cell lung cancer depending on the regulation of miR-512-3p/CORO1C

Heng Zhang¹ | Ting Huang² | Shisi Yuan¹ | Yuxi Long³ | Shuai Tan³ |
Guoliang Niu³ | Puhua Zhang³ | Meiling Yang³ 

¹The Affiliated Nanhua Hospital, Department of Hematology, Hengyang Medical School, University of South China, Hengyang, China

²The Affiliated Nanhua Hospital, Department of Pain Treatment, Hengyang Medical School, University of South China, Hengyang, China

³The Affiliated Nanhua Hospital, Department of Oncology, Hengyang Medical School, University of South China, Hengyang, China

Correspondence

Meiling Yang, The Affiliated Nanhua Hospital, Department of Oncology, Hengyang Medical School, University of South China, No. 336, Dongfeng South Road, Zhuhui District, Hengyang City, Hunan Province, 421001, PR China.
Email: nhhematology@163.com

Abstract

Background: Non-small cell lung cancer (NSCLC) is one of the leading causes responsible for cancer-associated death globally. The aim of this study was to illustrate the function of circular RNA_0020123 (circ_0020123) in NSCLC progression and its associated mechanism.

Methods: RNA and protein expression was determined by reverse transcription-quantitative polymerase chain reaction (RT-qPCR) and western blot assay. Cell proliferation, migration, invasion, angiogenesis, apoptosis and autophagy were analyzed to assess the role of circ_0020123/microRNA-512-3p (miR-512-3p)/coronin 1C (CORO1C) axis in NSCLC cells. Tumorigenesis in nude mice was analyzed to determine the in vivo role of circ_0020123. The intermolecular target relation was confirmed by dual-luciferase reporter and RNA immunoprecipitation (RIP) assays.

Results: Circ_0020123 expression was aberrantly upregulated in NSCLC tissues and cell lines. Circ_0020123 interference markedly restrained cell proliferation, migration, invasion, angiogenesis and autophagy and induced cell apoptosis of NSCLC cells. Circ_0020123 knockdown suppressed xenograft tumor growth in vivo. Circ_0020123 acted as a molecular sponge for miR-512-3p. Circ_0020123 silencing-induced effects in NSCLC cells were largely reversed by the knockdown of miR-512-3p. miR-512-3p interacted with the 3' untranslated region (3'UTR) of CORO1C. CORO1C overexpression largely reversed miR-512-3p accumulation-induced influences in NSCLC cells. Circ_0020123 positively regulated CORO1C expression by sponging miR-512-3p in NSCLC cells.

Conclusion: Circ_0020123 aggravated NSCLC progression by binding to miR-512-3p to induce CORO1C expression, which provided new potential targets for the treatment of NSCLC.

KEYWORDS

angiogenesis, circ_0020123, CORO1C, miR-512-3p, non-small cell lung cancer

INTRODUCTION

Non-small cell lung cancer (NSCLC) is a predominant pathological subtype in lung cancer.¹ The clinical symptoms of NSCLC are nontypical and insidious in the early stages, which causes a low detective rate for NSCLC patients.² The

overall five-year survival rate of NSCLC is about 16%.³ The factors involved in the initiation and progression of NSCLC are complicated, and uncovering the molecular mechanism behind NSCLC pathogenesis is beneficial for NSCLC treatment.

Circular RNAs (circRNAs) are endogenous single-stranded circular RNA molecules originally considered to be the byproducts during the process of RNA splicing.⁴ The

Heng Zhang and Ting Huang contributed equally to this work.

This is an open access article under the terms of the [Creative Commons Attribution-NonCommercial-NoDerivs](https://creativecommons.org/licenses/by-nc-nd/4.0/) License, which permits use and distribution in any medium, provided the original work is properly cited, the use is non-commercial and no modifications or adaptations are made.

© 2022 The Authors. *Thoracic Cancer* published by China Lung Oncology Group and John Wiley & Sons Australia, Ltd.

expression pattern of circRNAs is tissue-specific, and the dysregulation of circRNAs is associated with the pathogenesis of human diseases.^{5,6} Due to the stable structure and dysregulated expression of circRNAs in human malignancies, circRNAs are ideal biomarkers for human malignancies.⁷ For instance, in a previous study, circ_0000745 expression was found to be reduced in gastric cancer (GC) tissues and plasma samples, and low abundance of circ_0000745 was associated with poor indicators in GC patients, suggesting that circ_0000745 is a potential diagnostic marker for GC.⁸ Previous studies have demonstrated that circ_0020123 plays an oncogenic role in NSCLC.^{9–12} In this study, the working mechanism of circ_0020123 in NSCLC was further studied.

MicroRNAs (miRNAs) regulate multiple cellular behavior of tumor cells, including cell proliferation, migration, invasion and drug resistance.^{13,14} CircRNAs function as molecular sponges for miRNAs in human malignancies.¹⁵ Through bioinformatic prediction, miR-512-3p was found to be a potential target of circ_0020123. miR-512-3p abundance was declined in NSCLC specimens, and restrained cell adhesion and motility in NSCLC cells in a previous study.¹⁶ We testified that there is a binding relation between circ_0020123 and miR-512-3p and explored its functional relevance in NSCLC cells.

miRNAs possess the seed sequences that are complementary with the 3' untranslated region (3'UTR) of target messenger RNAs (mRNAs), and this combination causes degradation or the translational blockage of mRNAs.¹⁷ Coronin 1C (CORO1C) is a predicted target of miR-512-3p. A previous study highlighted that CORO1C is an interacted molecule of miR-206, and CORO1C contributes to NSCLC metastasis.¹⁸ The binding relationship between CORO1C and miR-512-3p and their regulatory relationship were explored in this study.

The expression characteristic and function of circ_0020123 in NSCLC were explored. The downstream target molecules of circ_0020123 were predicted through bioinformatic analysis, and rescue experiments were carried out to validate their functional relevance.

METHODS

Clinical tissue specimens

We collected NSCLC tissue samples and adjacent normal lung tissue samples from 39 NSCLC patients at The Affiliated Nanhua Hospital. All tumor tissues were histopathologically diagnosed as NSCLC. We collected blood samples from 39 NSCLC patients and 25 healthy volunteers. The blood samples were placed at 4°C for 1 h, and the serum fractions were separated by centrifugation at 3000 rpm for 5 min. The tissue and serum samples were stored at –80°C until use. Human materials were utilized with the supervision of the Ethics Committee of The Affiliated Nanhua Hospital and the signature of all participants in written informed consents.

Cell culture

A panel of NSCLC cell lines including A549, H1299 and PC-9, normal 16HBE cell line and human umbilical vein endothelial cell line (HUVEC) were provided by Shanghai Academy of Sciences (Shanghai, China). All cell lines were cultivated with Dulbecco's modified Eagle's medium (DMEM) medium (Gibco) with the supplement of 10% fetal bovine serum (FBS; Gibco) and 1% antibiotics (Sangon Biotech) in a humidified 37°C and 5% CO₂ condition.

Reverse transcription-quantitative polymerase chain reaction (RT-qPCR)

RNA samples in frozen tissues samples, serum samples, and cell lines were isolated with Trizol reagent (Invitrogen). The template DNA of mRNA and circRNA was acquired via a commercial RevertAid First-Strand cDNA Synthesis kit (Thermo Fisher Scientific), and the template of miRNA was obtained using the miRNA-specific forward primer and universal reverse primer (Ribobio). Template DNA was amplified using specific primers (Table 1) and SYBR Mix (Takara). Glyceraldehyde-3-phosphate dehydrogenase (GAPDH; to analyze circRNA and mRNA expression) or U6 (to detect miRNA expression) was set as internal reference. The fold change was evaluated using the equation of $2^{-\Delta\Delta C[T]}$.¹⁹

RNase R digestion

The circular feature of circ_0020123 was verified by exonuclease RNase R. RNAs were reacted with RNase R (100 µg/ml; Applied Biological Materials, Vancouver, Canada) at 37°C atmosphere for 30 min. RT-qPCR analysis was adopted for RNA determination.

TABLE 1 Specific primers in RT-qPCR assay

Gene	Direction	Sequence
circ_0020123	Forward	5'-GTATGCACTCTGGCCTGCTT-3'
	Reverse	5'-ACCCATCAGTTGACTGGACA-3'
PDZD8	Forward	5'-ACTAGTTTGGGCTGGTTTTGT-3'
	Reverse	5'-TGGGACCCGTAATAATGGACC-3'
miR-512-3p	Forward	5'-GCCGAGAAGTGCTGTCATAG-3'
	Reverse	5'-CTCAACTGGTGTCTGGA-3'
CORO1C	Forward	5'-ACCCTGGCCACGAATCATT-3'
	Reverse	5'-AACGCATGTGTGAAAGTGGC-3'
GAPDH	Forward	5'-CCTGTTCGACAGTCAGCCG-3'
	Reverse	5'-GAGAACAGTGAGCGCCTAGT-3'
U6	Forward	5'-GCTTCGGCAGCACATATACTAAAT-3'
	Reverse	5'-CGCTTCACGAATTTGCGTGTAT-3'

Abbreviation: PDZD8, PDZ domain containing 8.

Oligonucleotides and plasmids

Specific small interfering RNA (siRNA) molecule targeting circ_0020123 (si-circ_0020123), its corresponding negative control (si-NC), circ_0020123-specific short hairpin RNA (shRNA) (sh-circ_0020123), sh-NC, miR-512-3p-specific mimics (miR-512-3p), miR-NC, inhibitor of miR-512-3p (anti-miR-512-3p), anti-miR-NC, CORO1C overexpression plasmid in pcDNA3.1 vector (pcDNA3.1-CORO1C) and pcDNA3.1 were provided by Sangon Biotech and Genpharma (Shanghai, China). Commercial lipofectamine 3000 reagent (Invitrogen) was adopted during the cell transfection process.

Cell counting kit 8 (CCK8) assay

Transfected NSCLC cells (4×10^4 cells/well) were continued to culture for preset time points. CCK8 reagent (Dojindo) in 100 μ l medium was pipetted to the wells and reacted with cells. The optical density (OD) value at 450 nm was analyzed 4 h later.

5-Ethynyl-2'-deoxyuridine (EdU) assay

NSCLC cells were stimulated with 100 μ l medium plus 20 μ M EdU reagent (keyGEN BioTECH). After 2-h incubation, NSCLC cells were immobilized via 4% paraformaldehyde stationary liquid (Sangon Biotech) and mixed with 0.5% surfactant Triton-X-100 solution (Sangon Biotech). Cell nuclei was dyed using 4, 6-diamino-2-phenylindole dye liquor (DAPI; Sigma). The fluorescence signals were analyzed via a fluorescence microscope (Leica).

Transwell assays

NSCLC cells were plated onto the above transwell chambers (Costar, Corning) which were covered with (to analyze cell invasion ability) or without (to analyze cell migration ability) Matrigel reagent (BD Biosciences). The below chambers were filled with culture medium plus 10% FBS. NSCLC cells passed through the filter were dyed with 0.5% crystal violet dye liquor (Sangon Biotech). Images were captured at 100 \times .

Scratch assay

Transfected A549 cells were seeded onto 6-well plates to settle down. When cell confluence reached about 95%, scratches were created using 200 μ l pipette tip. Cells were washed twice to remove cell debris and floating cells. Cell images were taken at 0 and 24 h after creating the wounds. The wound width was analyzed by ImageJ software (National Institutes of Health).

Tube formation assay

The culture medium of transfected NSCLC cells was added to incubate with HUVECs in 96-well plates (2×10^4 cells/well) which were covered with Matrigel (BD Biosciences). At 10 h post cultivation, the number of branches in each node was counted.

Flow cytometry

NSCLC cells were suspended and synchronously stained using fluorescein isothiocyanate (FITC)-conjugated Annexin V (Becton) and propidium iodide (PI; Becton). Cell samples were loaded onto the FACS CantoII flow cytometer (BD Biosciences), and the ratio of cells with FITC⁺ and PI^{+/-} (apoptosis rate) was analyzed by BD FACSDiva software (BD Biosciences).

Western blot assay

Protein samples were prepared by radioimmunoprecipitation assay (RIPA) agentia (Sangon Biotech). Protein samples were separated by sodium dodecyl sulfate-polyacrylamide gel electrophoresis (SDS-PAGE) and were blotted onto a commercial polyvinylidene difluoride (PVDF) membrane (Bio-Rad). After sealing the nonspecific sites, diluted primary antibodies (Table 2) were then pipetted to incubate with the membrane at 4°C overnight. Subsequently, the membrane was incubated with the secondary antibody (Abcam). Immunoreactive protein signals were appeared using commercial enhanced chemiluminescence (ECL) reagent (Millipore).

Xenograft tumor model

Male nude mice (strain: BALB/c; Vital River Laboratory Animal Technology, Beijing, China) were grown in a sterile environment and arbitrarily divided into sh-NC group and sh-circ_0020123 group with five mice in each group. Phosphate buffer saline (PBS) solution (Sangon Biotech) was utilized to prepare A549 cell suspension (3×10^6 cells), and cell suspension was inoculated into the back of nude mice.

TABLE 2 Primary antibodies used in western blot assay

Antibody	Catalogue no.	Supplier
PCNA	ab29	Abcam, Cambridge, MA, USA
MMP9	ab76003	Abcam, Cambridge, MA, USA
Cleaved caspase 3	ab32042	Abcam, Cambridge, MA, USA
LC3 I/II	ab221794	Abcam, Cambridge, MA, USA
p62	ab109012	Abcam, Cambridge, MA, USA
CORO1C	SAB2500264	Sigma, St. Louis, MO, USA
GAPDH	Ab181602	Abcam, Cambridge, MA, USA

Tumor dimension was measured every 7 days using the formula of length \times width² \times 0.5. At 28 days post-injection, tumor weight was recorded. RT-qPCR was used to analyze circ_0020123 expression, and immunohistochemistry (IHC) experiment was adopted to analyze expression of proliferation marker molecule Ki67 in protein level. All procedures were authorized by the Animal Experimentation Ethics Committee of The Affiliated Nanhua Hospital.

Subcellular fractionation

The cytoplasmic and nuclear RNA contents were extracted via a PARIS Kit Protein and RNA Isolation system (Thermo Fisher Scientific). GAPDH and U6 were regarded as references for cytoplasm and nucleus.

Establishment of circRNA/miRNA/mRNA axis

The StarBase database was utilized to predict circRNA-miRNA interactions, whereas TargetScan database was adopted to predict miRNA-mRNA interactions.

Dual-luciferase reporter assay

The putative binding region with miR-512-3p in partial fragment of circ_0020123 or CORO1C was subcloned into

pmirGLO plasmid (Promega) to generate wild-type (WT)-circ_0020123 or WT-CORO1C 3'UTR. Meanwhile, mutant type (MUT) binding sequence in circ_0020123 or CORO1C was also inserted into pmirGLO plasmid (Promega) to construct MUT-circ_0020123 or MUT-CORO1C 3'UTR. NSCLC cells were cointroduced with reporter plasmids and miR-512-3p or miR-NC. Both Firefly and Renilla luciferase intensities were determined by commercial Dual-Luciferase Reporter Assay System Kit (Promega).

RNA immunoprecipitation (RIP) assay

Briefly, the magnetic beads in Magna RIP assay Kit (gzsbcio) and Argonaute2 (Ago2; Abcam) antibody or immunoglobulin G (IgG; Abcam) antibody were incubated with RNA samples. Afterwards, proteinase K was pipetted for RNA purification. The enriched RNAs were analyzed by RT-qPCR.

Statistical analysis

The differences in groups were assessed via GraphPad Prism 7.0 (GraphPad). The data were expressed as the form of mean \pm standard deviation (SD). The difference was assessed by Student's *t*-test or one-way analysis of variance (ANOVA). Values of *p* < 0.05 were considered statistically significant.

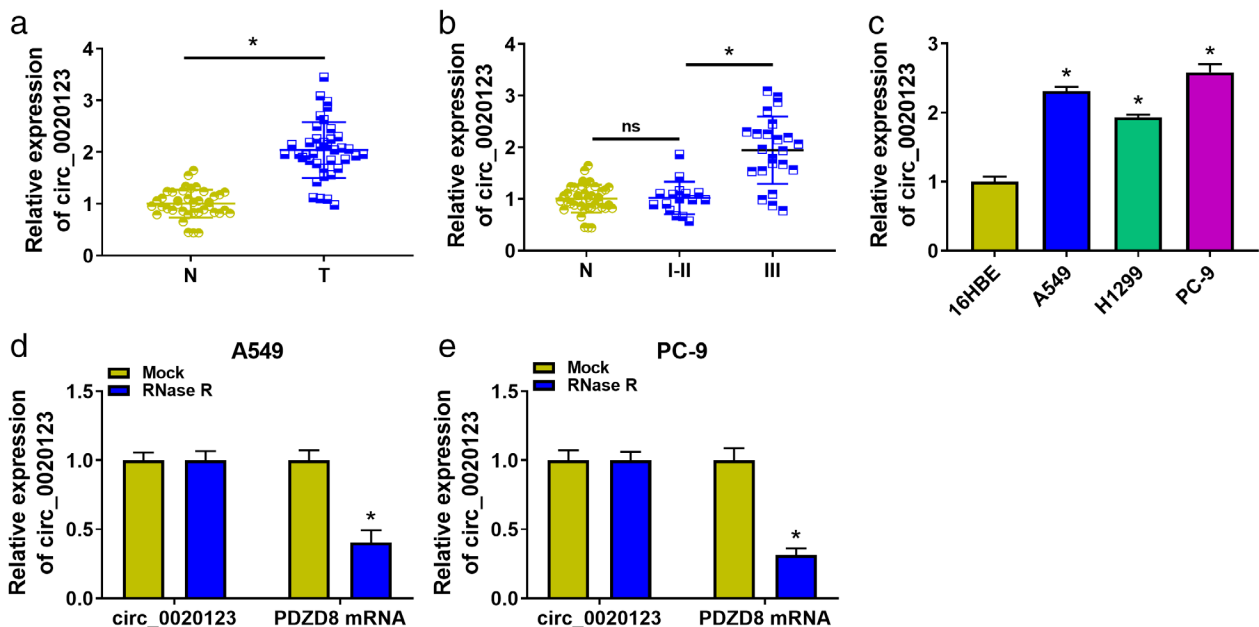


FIGURE 1 Circ_0020123 expression is upregulated in NSCLC tissues and cell lines. (a) RT-qPCR was applied to measure the expression of circ_0020123 in 39 pairs of NSCLC tissues and matched normal tissues. (b) Based on the TNM staging system, NSCLC patients were divided into I-II phase ($n = 16$) and III phase ($n = 23$). The expression of circ_0020123 in tumor tissues in two groups was shown. (c) RT-qPCR was adopted to analyze the expression of circ_0020123 in 16HBE and three NSCLC cell lines, including A549, H1299 and PC-9. (d and e) The RNase R resistance of circ_0020123 and its linear form PDZD8 mRNA was tested by RT-qPCR. * $p < 0.05$

RESULTS

Circ_0020123 expression is upregulated in NSCLC tissues and cell lines

We first analyzed the expression pattern of circ_0020123 in NSCLC tissues and adjacent normal tissues. Circ_0020123

was highly expressed in NSCLC tumor tissues ($n = 39$) relative to that in matched normal tissues ($n = 39$) (Figure 1a). NSCLC patients were divided into I–II phase ($n = 16$) and III phase ($n = 23$) according to the tumor-lymph node metastasis (TNM) staging system. There was no significant difference in the expression of circ_0020123 in adjacent normal tissues and tumor tissues (stage I–II) (Figure 1b),

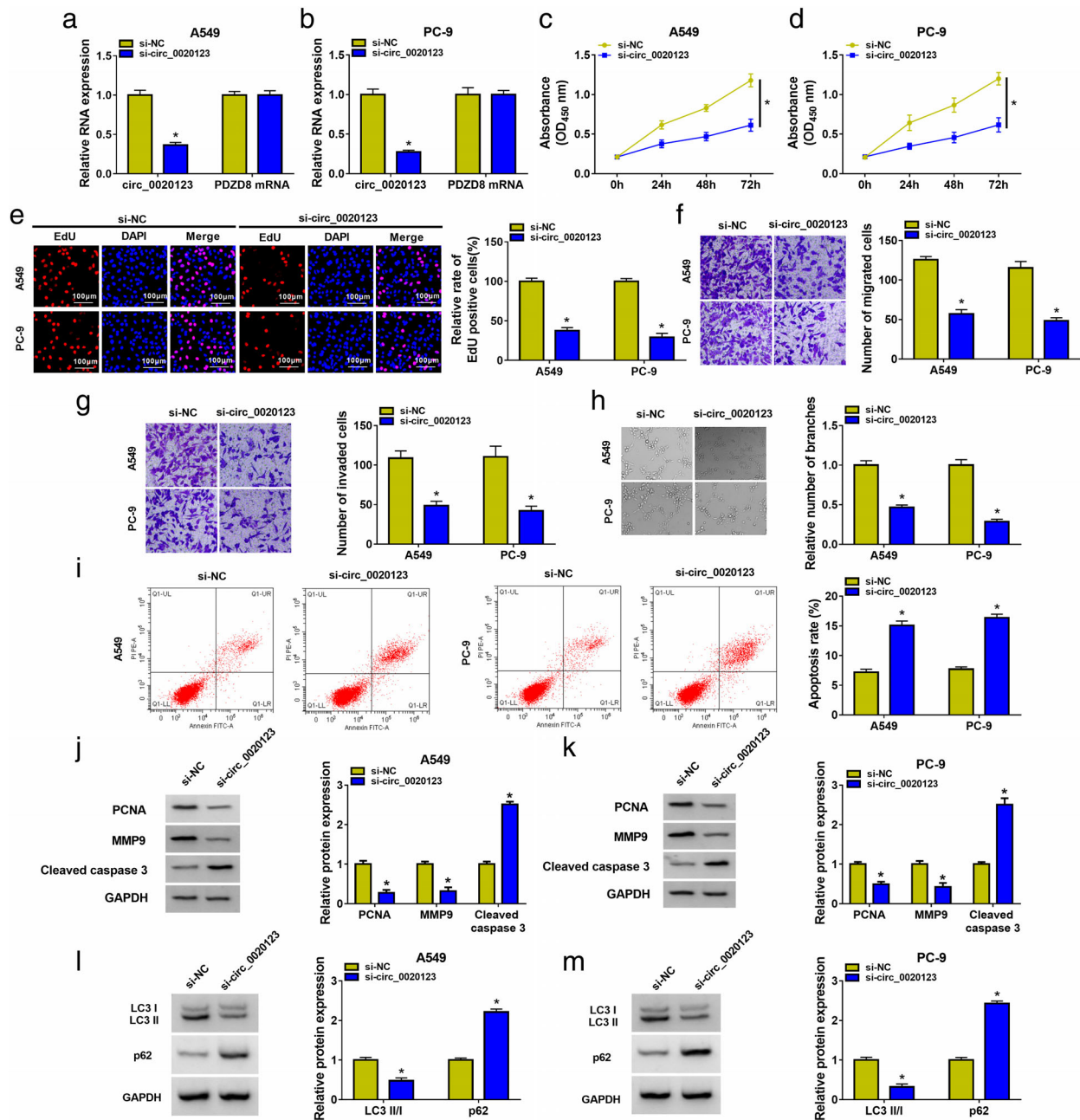


FIGURE 2 Circ_0020123 silencing restrains cell proliferation, migration, invasion, angiogenesis and autophagy whereas triggers cell apoptosis in NSCLC cells. (a and b) The silencing efficiency and specificity of si-circ_0020123 in NSCLC cells were tested by RT-qPCR. (c–m) NSCLC cells were transfected with si-NC or si-circ_0020123. (c and d) Cell proliferation curve was generated through CCK8 assay. (e) The incorporation of EdU was monitored by EdU assay to analyze cell proliferation. (f and g) Cell motility capacity, including migration and invasion abilities, was analyzed by transwell assays. (h) Cell angiogenesis was evaluated by tube formation assay. (i) Cell apoptosis rate (FITC⁺ and PI^{+/-}) was analyzed by flow cytometry. (j and k) Western blot assay was performed to examine the protein levels of proliferation-, motility-, and apoptosis-related markers (PCNA, MMP9, and cleaved caspase3) in transfected NSCLC cells. (l and m) cell autophagy was assessed through measuring the levels of LC3 I, LC3 II and p62 via western blot assay. * $p < 0.05$

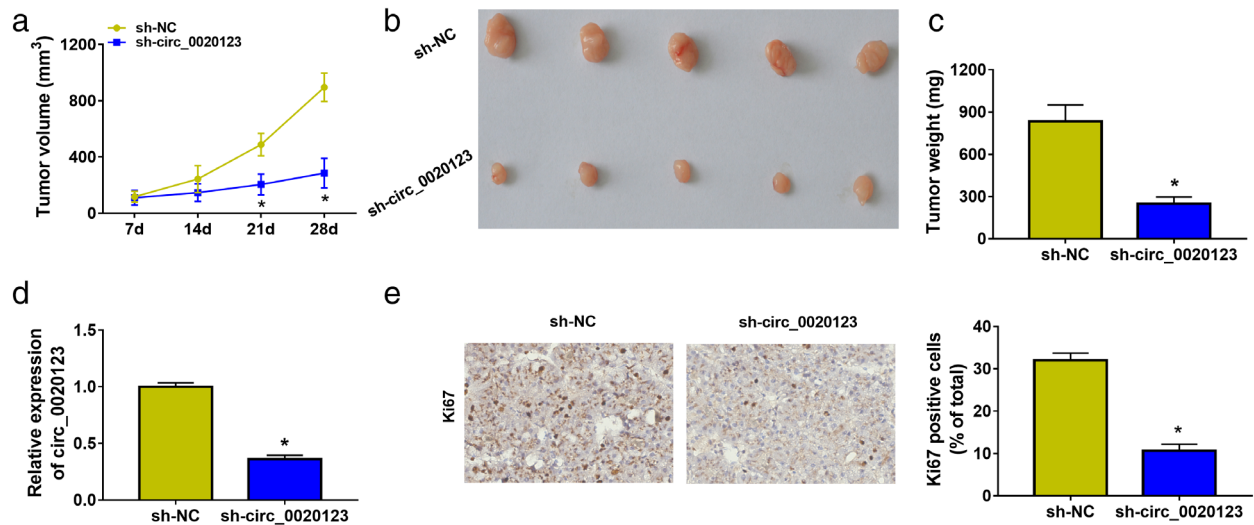


FIGURE 3 Circ_0020123 interference markedly suppresses tumor progression in vivo. Nude mice were inoculated with A549 cells stably transfected with sh-NC ($n = 5$) or sh-circ_0020123 ($n = 5$). (a) Tumor volume was measured every 7 days for 28 days. (b and c) After inoculation for 28 days, all nude mice were euthanized and the xenograft tumors were resected, imaged, and weighed. (d) RT-qPCR was applied to measure the expression of circ_0020123 in tumor tissues. (e) IHC assay was implemented to analyze the protein level of proliferation marker Ki67 in tumor tissues. $*p < 0.05$

suggesting that circ_0020123 could not be a sensitive early biomarker for the diagnosis of NSCLC. We found that NSCLC patients with advanced tumor stage tended to have high circ_0020123 expression (Figure 1b), suggesting that circ_0020123 might be an effective therapeutic target to prevent the progression of NSCLC. We found that circ_0020123 was upregulated in the serum samples of NSCLC patients compared with healthy volunteers (Figure S1a), and its level in serum samples was positively correlated with the TNM staging of tumors (Figure S1b), which was consistent with its expression in tissue samples. Circ_0020123 expression was elevated in NSCLC cell lines compared with 16HBE cell line (Figure 1c). We then tested if circ_0020123 was a circular transcript using exonuclease RNase R that only degraded linear RNAs with 3' terminal end, and the linear counterpart PDZ domain containing 8 (PDZD8) was used as the control. RNase R digestion almost did not affect circ_0020123 expression (Figures 1d,e), suggesting that circ_0020123 was resistant to RNase R digestion. The level of linear PDZD8 mRNA was markedly reduced upon RNase R digestion (Figures 1d,e). These results implied that abnormal upregulation of circ_0020123 expression might be associated with the malignant progression of NSCLC.

Circ_0020123 silencing restrains cell proliferation, migration, invasion, angiogenesis and autophagy whereas triggers cell apoptosis in NSCLC cells

Given the abnormal upregulation of circ_0020123 in NSCLC cells, we aimed to analyze the potential biological significance behind the aberrant expression of circ_0020123. Prior to perform loss-of-function experiments, we assessed

the silencing efficiency of circ_0020123 along with its specificity. Transfection with si-circ_0020123 markedly reduced circ_0020123 expression rather than its linear form PDZD8 mRNA in NSCLC cells (Figure 2a,b). Circ_0020123 knockdown suppressed the proliferation of NSCLC cells (Figure 2c,d). The incorporation of EdU was notably reduced by circ_0020123 silencing (Figure 2e), indicating that circ_0020123 interference inhibited the proliferation of NSCLC cells. We found that both the numbers of migrated and invaded cells were decreased in circ_0020123-silenced group (Figure 2f,g), which manifested that circ_0020123 silencing restrained the motility of NSCLC cells. We conducted scratch assay to further confirm the role of circ_0020123 in regulating cell migration. The data showed that circ_0020123 knockdown blocked the closure of the wound compared with si-NC group (Figure S1g), further suggesting that circ_0020123 knockdown suppressed the migration of NSCLC cells. We then analyzed the angiogenesis ability of NSCLC cells through tube formation assay. As shown in Figure 2h, circ_0020123 knockdown led to a significant reduction in the number of branches, indicating that circ_0020123 silencing suppressed the tube formation ability of NSCLC cells. Circ_0020123 knockdown induced the apoptosis of NSCLC cells (Figure 2i). To further confirm the roles of circ_0020123 on the proliferation, motility, and apoptosis of NSCLC cells, we detected the protein levels of PCNA, MMP9, and cleaved caspase3 in circ_0020123-silenced NSCLC cells. The data revealed that circ_0020123 knockdown reduced the protein levels of PCNA and MMP9 while elevated the protein level of cleaved caspase3 (Figure 2j,k), further indicating that circ_0020123 absence suppressed the proliferation and motility and induced the apoptosis of NSCLC cells. LC3 is a vital molecular marker during autophagy activation. The conversion of LC3 I to LC3 II denotes the activation of autophagy. P62 is an adaptor protein that binds to LC3 II, and it is also an

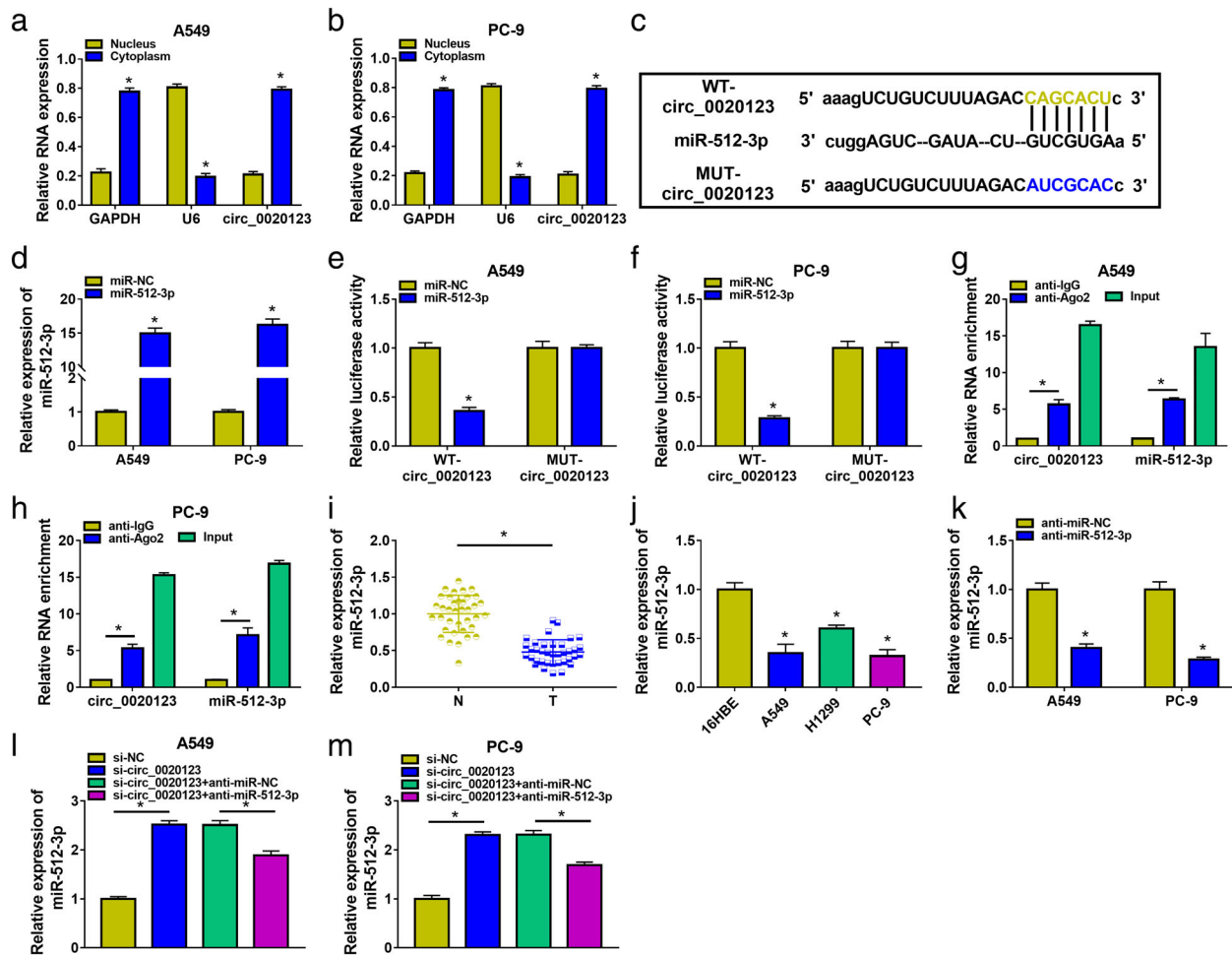


FIGURE 4 Circ_0020123 serves as a sponge for miR-512-3p in NSCLC cells. (a and b) The subcellular localization of circ_0020123 was analyzed. (c) StarBase database predicted the binding sites between circ_0020123 and miR-512-3p. (d) RT-qPCR was applied to verify the overexpression efficiency of miR-512-3p in NSCLC cells. (e and f) Dual-luciferase reporter assay was applied to confirm the target relation between circ_0020123 and miR-512-3p. (g and h) RIP assay was implemented to verify the spatial interaction between circ_0020123 and miR-512-3p in RISC. (i) RT-qPCR was conducted to detect the level of miR-512-3p in NSCLC tumor tissues ($n = 39$) and adjacent normal tissues ($n = 39$). (j) The expression of miR-512-3p in NSCLC cell lines (A549, H1299 and PC-9) and 16HBE was determined by RT-qPCR. (k) The interference efficiency of anti-miR-512-3p in NSCLC cells was tested via RT-qPCR. (l and m) A549 and PC-9 cells were transfected with si-circ_0020123 alone or together with anti-miR-512-3p, and the level of miR-512-3p was determined by RT-qPCR. * $p < 0.05$

important molecular marker in autophagy. The level of LC3 II/LC3 I was reduced whereas p62 level was increased by circ_0020123 silencing (Figure 2l,m), suggesting that circ_0020123 knockdown suppressed the autophagy of NSCLC cells. 16HBE cells were transfected with si-NC or si-circ_0020123, and we found that cell proliferation ability of 16HBE cells was unaffected by silencing circ_0020123 (Figure S1c). These results revealed that circ_0020123 knockdown could only influence the biological behaviors of NSCLC cells but not that of normal cells, suggesting the different sensitivity of circ_0020123 between cancer cells and normal cells. We detected the expression of proliferation-related protein (PCNA), metastasis-associated protein (MMP9), and autophagy-related protein (LC3 I, LC3 II, and p62) in A549, 16HBE, NSCLC tissues, and adjacent normal tissues. The data showed that the levels of PCNA, MMP9, and LC3 II/I were upregulated in A549 and NSCLC tissues

compared with 16HBE and adjacent normal tissues, while the expression of p62 exhibited an opposite tendency to these molecules (Figure S1d,e). Taken together, circ_0020123 knockdown restrained the malignant phenotypes and promoted the apoptosis of NSCLC cells.

Circ_0020123 interference markedly suppresses tumor progression in vivo

We intended to verify whether circ_0020123 exerted a protumor activity in vivo, and xenograft tumor model was used. Tumor growth curve was drawn through monitoring tumor volume for 28 days. Circ_0020123 knockdown notably suppressed xenograft tumor growth (Figure 3a). Tumor weight was markedly reduced in sh-circ_0020123 group relative to that in sh-NC group (Figure 3b,c). The expression

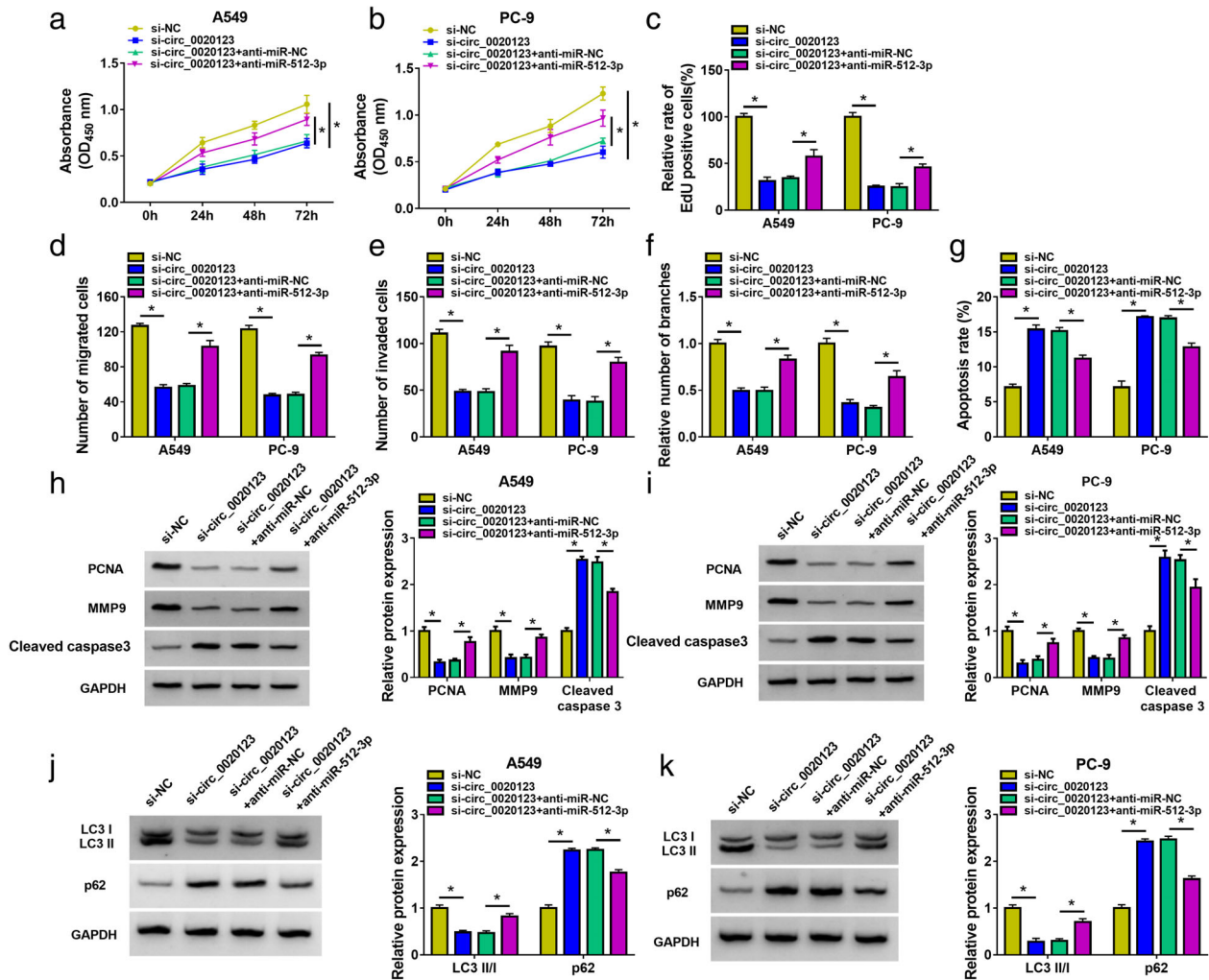


FIGURE 5 Circ_0020123 silencing-induced effects are largely overturned by miR-512-3p knockdown in NSCLC cells. (a–k) A549 and PC-9 cells were introduced with si-circ_0020123 alone or together with anti-miR-512-3p. (a and b) CCK8 assay was applied to determine cell proliferation ability. (c) Cell proliferation ability was analyzed by EdU assay. (d and e) Transwell assays were conducted to evaluate cell migration and invasion abilities. (f) Tube formation assay was adopted to analyze cell tube formation ability. (g) Cell apoptosis rate was tested by flow cytometry. (h and i) The protein levels of PCNA, MMP9, and cleaved caspase3 in transfected NSCLC cells were determined by western blot assay. (j and k) Western blot assay was used to detect the expression of autophagy-associated proteins (LC3 I, LC3 II and p62) in transfected NSCLC cells. * $p < 0.05$

of circ_0020123 was reduced in sh-circ_0020123 group compared with sh-NC group (Figure 3d). Based on IHC assay, we found that proliferation-associated marker Ki67 was downregulated in tumor tissues with the knockdown of circ_0020123 than that in sh-NC group (Figure 3e). Circ_0020123 knockdown reduced the levels of PCNA, MMP9, and LC3 II/I and elevated the protein expression of p62 in xenograft tumor tissues (Figure S1f). Overall, circ_0020123 knockdown notably restrains xenograft tumor growth.

Circ_0020123 serves as a sponge for miR-512-3p in NSCLC cells

Circ_0020123 was majorly located in the cytoplasmic fraction of NSCLC cells (Figure 4a,b), implying that circ_0020123

might function by sponging miRNAs. The potential binding sites with circ_0020123 in miR-512-3p were predicted by the StarBase database (<http://starbase.sysu.edu.cn>) (Figure 4c). Transfection efficiency of miR-512-3p mimics in NSCLC cells was verified via RT-qPCR assay (Figure 4d). With the overexpression of miR-512-3p, the luciferase activity of WT-circ_0020123 was dramatically declined compared with that in miR-NC and WT-circ_0020123 group (Figures 4e,f), suggesting the binding relation between circ_0020123 and miR-512-3p. However, luciferase intensity of MUT-circ_0020123 remained unaffected by the transfection of miR-NC or miR-512-3p (Figures 4e,f), manifesting that miR-512-3p interacted with circ_0020123 via the putative sites. As indicated in Figures 4g,h, circ_0020123 and miR-512-3p were both pulled down in the Ago2 antibody group, suggesting the spatial binding relation between circ_0020123 and miR-512-3p. miR-512-3p expression was reduced in NSCLC

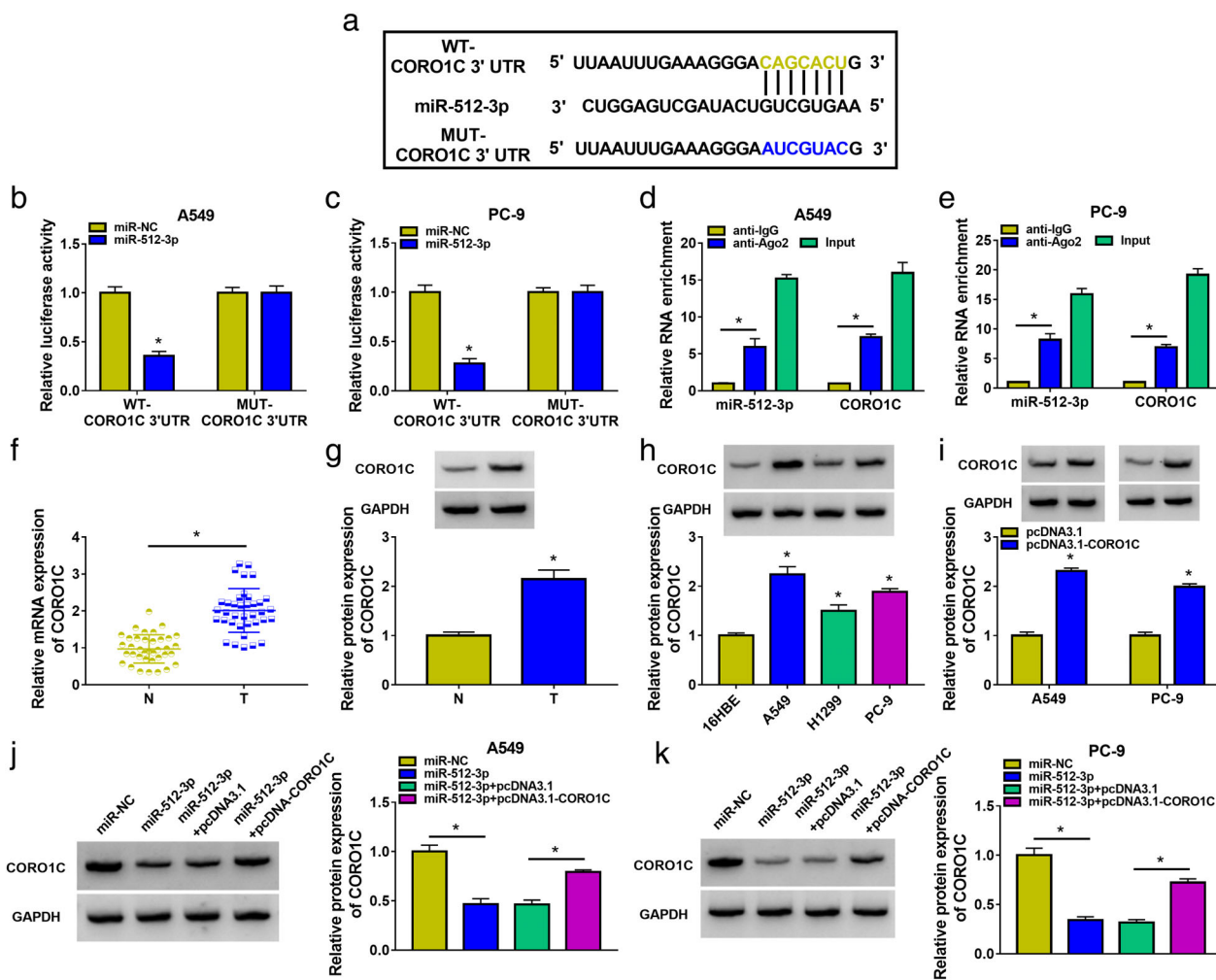


FIGURE 6 CORO1C is a target of miR-512-3p in NSCLC cells. (a) The binding sequence between miR-512-3p and CORO1C was predicted by TargetScan database. (b and c) The binding relation between miR-512-3p and CORO1C was tested via dual-luciferase reporter assay. (d and e) RIP assay was employed to confirm the target relation between miR-512-3p and CORO1C. (f and g) RT-qPCR and western blot assay were utilized to measure the expression of CORO1C in NSCLC tissues and adjacent normal tissues in mRNA and protein levels. (h) Western blot assay was utilized to measure the protein level of CORO1C in NSCLC cell lines and 16HBE cell line. (i) The overexpression efficiency of CORO1C ectopic expression plasmid was analyzed by western blot assay. (j and k) The protein level of CORO1C was determined in NSCLC cells transfected with the following four groups by western blot assay: miR-NC, miR-512-3p, miR-512-3p + pcDNA3.1 and miR-512-3p + pcDNA3.1-CORO1C. * $p < 0.05$

tissues and cell lines in comparison with that in adjacent normal tissues and 16HBE cell line (Figure 4i,j). RT-qPCR assay verified the high silencing efficiency of anti-miR-512-3p in NSCLC cells (Figure 4k). Circ_0020123 knockdown upregulated miR-512-3p expression, and the introduction of anti-miR-512-3p reduced miR-512-3p level again in NSCLC cells (Figure 4l,m). Overall, miR-512-3p was a target of circ_0020123 in NSCLC cells.

Circ_0020123 silencing-induced effects are largely overturned by miR-512-3p knockdown in NSCLC cells

To analyze if circ_0020123 silencing suppressed the malignant behaviors of NSCLC cells by upregulating its target miR-512-3p, we carried out compensation experiments

through transfecting NSCLC cells with si-circ_0020123 alone or together with anti-miR-512-3p. The silencing of miR-512-3p largely rescued the proliferation of circ_0020123-silenced NSCLC cells, as evidenced by the results of CCK8 assay and EdU assay (Figures 5a–c). Circ_0020123 interference-induced suppressive effects in the migration and invasion of NSCLC cells were largely diminished by miR-512-3p knockdown (Figures 5d,e). The angiogenesis ability of NSCLC cells was suppressed by circ_0020123 silencing, which was largely reversed by miR-512-3p knockdown (Figure 5f). Circ_0020123 silencing-induced apoptosis in NSCLC cells was also largely attenuated by the addition of anti-miR-512-3p (Figure 5g). The changes in the protein levels of PCNA, MMP9, and Cleaved caspase3 mediated by circ_0020123 absence were largely reversed by miR-512-3p knockdown (Figure 5h,i). The level of LC3 II/LC3 I was partly recovered by the introduction of anti-miR-512-3p

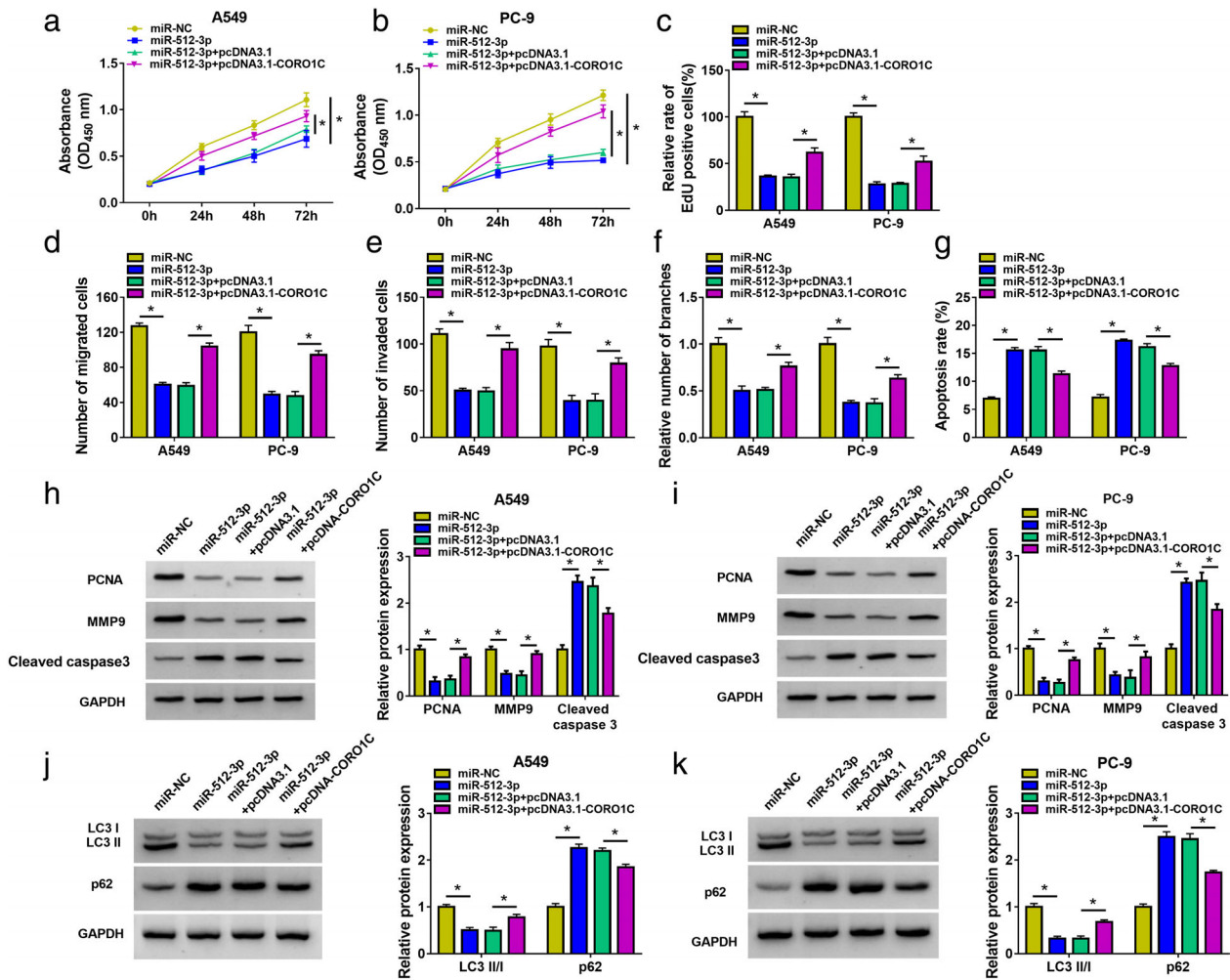


FIGURE 7 miR-512-3p overexpression restrains the malignant behaviors of NSCLC cells partly by downregulating its target CORO1C. (a–k) NSCLC cells were introduced with miR-512-3p alone or together with CORO1C ectopic expression plasmid. (a and b) Cell proliferation capacity was determined by CCK8 assay. (c) EdU assay was implemented to assess cell proliferation ability. (d and e) Cell motility was analyzed by transwell assays. (f) The tube formation ability of NSCLC cells was tested via tube formation assay. (g) Flow cytometry was adopted to evaluate the apoptosis rate of transfected NSCLC cells. (h and i) Western blot assay was carried out to examine the protein levels of PCNA, MMP9, and cleaved caspase3 in transfected NSCLC cells. (j and k) The protein levels of autophagy-associated proteins (LC3 I, LC3 II and p62) in NSCLC cells were detected by western blot assay. * $p < 0.05$

(Figures 5j,k). The expression of p62 exhibited an opposite tendency to LC3 II/LC3 I (Figures 5j,k). These results suggested that circ_0020123 interference suppressed malignant phenotypes and triggered the apoptosis of NSCLC cells partly by upregulating miR-512-3p.

CORO1C is a target of miR-512-3p in NSCLC cells

Based on bioinformatics prediction using TargetScan database (<http://www.targetscan.org>), CORO1C was a potential target of miR-512-3p in NSCLC cells. The putative binding sites between miR-512-3p and CORO1C were shown in Figure 6a. Transfection with miR-512-3p mimics caused a notable reduction in the luciferase activity of WT-CORO1C 3'UTR plasmid rather than MUT-CORO1C 3'UTR (Figure 6b,c), indicating that CORO1C was a target of miR-

512-3p in NSCLC cells. Both miR-512-3p and CORO1C were enriched in Ago2 antibody group (Figure 6d,e), demonstrating the spatial interaction between miR-512-3p and CORO1C in RNA-induced silencing complex (RISC). The mRNA and protein levels of CORO1C were upregulated in NSCLC tissues relative to normal tissue specimens (Figure 6f,g). Also, we found that CORO1C protein expression was enhanced in NSCLC cell lines compared with 16HBE cell line (Figure 6h). Transfection with CORO1C overexpression plasmid markedly increased its protein level in NSCLC cells (Figure 6i). miR-512-3p overexpression reduced CORO1C protein level in NSCLC cells (Figure 6j,k), suggesting that miR-512-3p negatively regulated CORO1C expression. Then, we performed compensation experiments through cotransfection of NSCLC cells with miR-512-3p and pcDNA3.1-CORO1C to rescue the expression of CORO1C (Figure 6j,k). We transfected anti-miR-NC or anti-miR-512-3p into 16HBE cells and found that the protein expression of CORO1C was notably upregulated

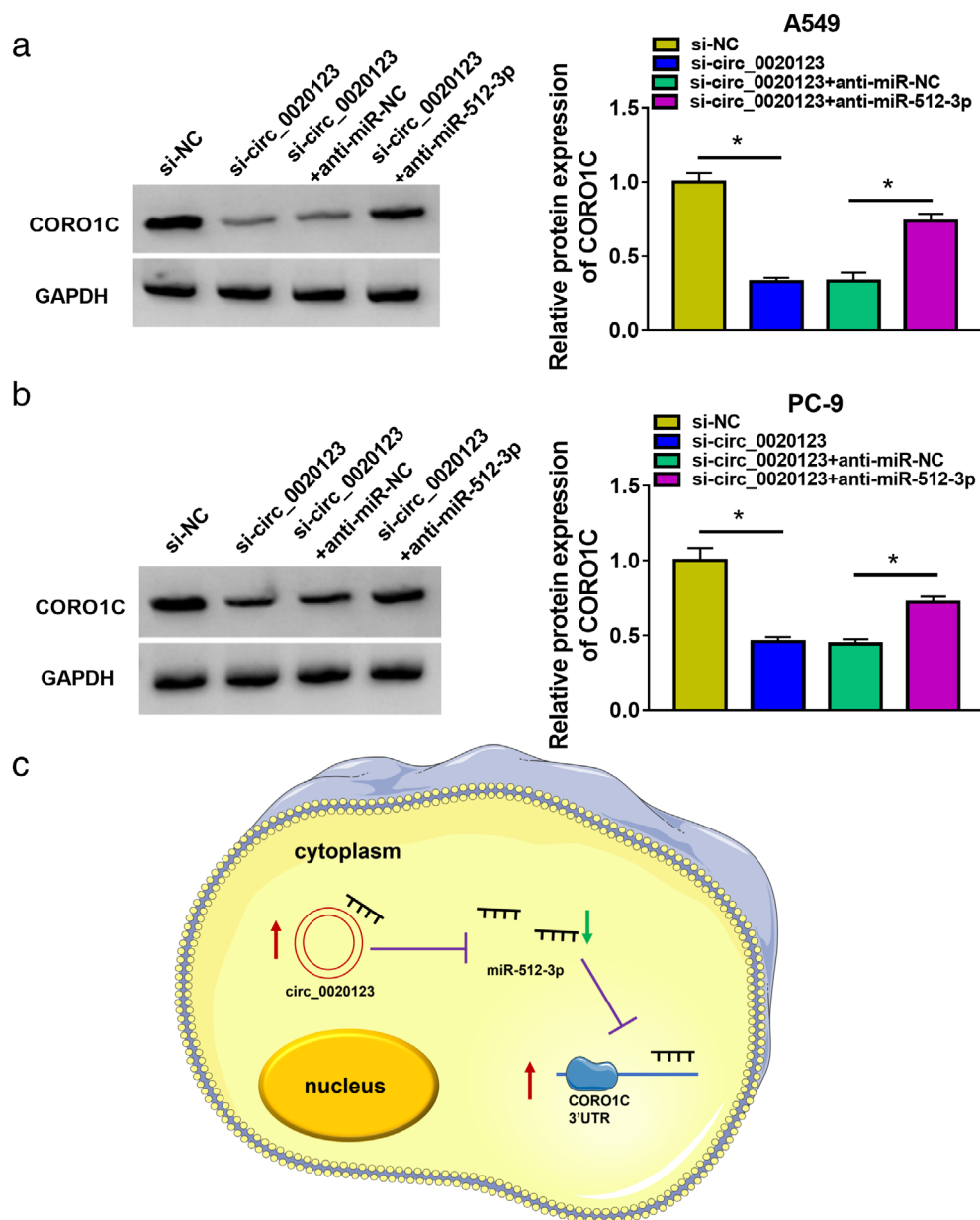


FIGURE 8 Circ_0020123 acts as miR-512-3p sponge to upregulate CORO1C expression in NSCLC cells. (a and b) A549 and PC-9 cells were transfected with si-circ_0020123 alone or together with anti-miR-512-3p. Western blot assay was adopted to measure the protein level of CORO1C in transfected NSCLC cells. (c) Circ_0020123 can act as a molecular sponge of miR-512-3p to upregulate the expression of CORO1C in NSCLC cells, thereby leading to the changes in cell biological behaviors. * $p < 0.05$

in the miR-512-3p-silenced group compared with the anti-miR-NC group (Figure S1h), suggesting that miR-512-3p/CORO1C regulatory axis was also existed in 16HBE cells. Overall, miR-512-3p negatively regulated CORO1C expression by binding to it in NSCLC cells.

miR-512-3p overexpression restrains the malignant behaviors of NSCLC cells partly by downregulating its target CORO1C

miR-512-3p overexpression prominently restrained the proliferation ability of NSCLC cells (Figure 7a,c). In addition, we found that miR-512-3p overexpression also inhibited the migration, invasion, tube formation and autophagy and triggered the apoptosis of NSCLC cells (Figure 7d,k). These

results further demonstrated the anti-tumor activity of miR-512-3p in NSCLC cells. With the addition of CORO1C plasmid, cell proliferation was largely recovered (Figure 7a-c). Cell migration and invasion abilities were also largely rescued in miR-512-3p and CORO1C plasmid co-transfected group (Figure 7d,e). The tube formation ability was restrained by miR-512-3p overexpression, which was largely rescued by the addition of pcDNA3.1-CORO1C (Figure 7f). miR-512-3p overexpression-induced apoptosis in NSCLC cells was also largely attenuated by CORO1C overexpression (Figure 7g). miR-512-3p overexpression downregulated the protein levels of PCNA and MMP9 and increased the protein level of cleaved caspase3, and these effects were largely offset by CORO1C accumulation (Figure 7h,i), further suggesting that miR-512-3p overexpression restrained the proliferation and motility and triggered the apoptosis of

NSCLC cells largely by downregulating CORO1C. The introduction of CORO1C plasmid also increased LC3 II/LC3 I level and reduced the level of p62 in NSCLC cells (Figure 7j,k), manifesting that CORO1C overexpression promoted the autophagy of NSCLC cells. These findings together suggested that miR-512-3p restrained NSCLC progression largely by targeting CORO1C.

Circ_0020123 acts as miR-512-3p sponge to upregulate CORO1C expression in NSCLC cells

Given the negative regulatory relation between miR-512-3p and circ_0020123 or CORO1C, we further analyzed the regulation among circ_0020123, miR-512-3p and CORO1C in NSCLC cells. Circ_0020123 knockdown prominently reduced CORO1C expression, and CORO1C expression was largely recovered by the addition of anti-miR-512-3p in NSCLC cells (Figure 8a,b). The schematic diagram showed the role of circ_0020123 on the regulation of miR-512-3p/CORO1C axis in NSCLC cells. Circ_0020123 could upregulate the expression of CORO1C by sequestering miR-512-3p in NSCLC cells (Figure 8c).

DISCUSSION

Deep understanding of the molecular mechanism behind NSCLC progression is necessary to find novel therapeutic targets. CircRNAs were originally thought to be the byproducts during the RNA shearing process.⁴ With the development of sequencing technology and bioinformatic analysis, a growing number of circRNAs have been identified, and the association between dysregulated circRNAs and tumor pathogenesis has received more and more attention.^{20,21} Circ_0020123 has been identified to be an oncogene in NSCLC in previous studies.^{9–12} For instance, Qu et al.⁹ demonstrated that circ_0020123 abundance was enhanced in NSCLC, and high abundance of circ_0020123 was associated with aggressive phenotypes of tumors and malignant behaviors of NSCLC cells. Wan et al.¹¹ demonstrated that circ_0020123 aggravated NSCLC development by mediating miR-488-3p/ADAM9 axis. Consistently, circ_0020123 abundance is found to be elevated in NSCLC. High levels of circ_0020123 are closely correlated with advanced TNM tumor stage in NSCLC patients. We also demonstrated that circ_0020123 knockdown suppressed proliferation, migration, invasion and angiogenesis and induced the apoptosis of NSCLC cells.

Cell autophagy can be induced by multiple factors, including nutrient starvation, hypoxic stress and other conditions.²² Previous studies have pointed out the pivotal role of autophagy in maintaining the survival of cancer cells under stress conditions.²³ Suppressing cell autophagy has previously been reported to induce the death of cancer cells.²⁴ Herein, we analyzed the role of circ_0020123 in regulating cell autophagy of NSCLC cells. After silencing circ_0020123, we found that cell autophagy of NSCLC cells

was suppressed. Through a xenograft tumor model, we found that circ_0020123 knockdown restrained tumor growth in vivo.

CircRNAs can serve as miRNA sponges to suppress their functions.¹⁵ Circ_0000376 has previously been reported to promote the proliferation, motility and drug resistance of NSCLC cells by acting as miR-384 sponge.²⁵ In one study, circ_0078767 restrained the malignant behaviors of NSCLC cells by targeting miR-330-3p.²⁶ Using the StarBase bioinformatic database, we found that miR-512-3p harbored a potential binding sequence with circ_0020123. miR-512-3p has also been identified as a tumor suppressor in multiple malignancies, including prostate cancer,²⁷ triple-negative breast cancer,²⁸ colorectal cancer²⁹ and NSCLC.^{16,30} Zhu et al.¹⁶ demonstrated that miR-512-3p hampered malignant phenotypes in NSCLC cells by modulating DOCK3/RAC1. Zhang et al.³⁰ demonstrated that MAGI1-IT1 contributed to NSCLC progression by elevating AKT1 expression via sponging miR-512-3p, suggesting the tumor suppressor role of miR-512-3p in NSCLC. A target relationship between circ_0020123 and miR-512-3p has been verified, and we found that circ_0020123 interference restrained the malignant behaviors of NSCLC cells partly by upregulating miR-512-3p.

miRNAs bind to their target mRNAs to regulate the stability and translation of mRNAs.³¹ CORO1C has been verified to be a target of miR-512-3p. CORO1C plays a pivotal regulatory role for cell motility by actin filament turnover coordination.³² Accumulating studies have found that CORO1C expression is aberrantly upregulated in many aggressive malignancies, including triple-negative breast cancer³³ and gastric cancer.³⁴ In NSCLC, Liao et al.¹⁸ demonstrated that miR-206 restrained the proliferation and motility of NSCLC cells by targeting CORO1C. CORO1C was found to be significantly upregulated in NSCLC tissues and cell lines. miR-512-3p overexpression inhibited the malignant behaviors of NSCLC cells, and these effects were largely reversed by the overexpression of CORO1C, suggesting that miR-512-3p functioned partly by targeting CORO1C in NSCLC cells. Circ_0020123 served as an miR-512-3p sponge to upregulate CORO1C expression in NSCLC cells.

In summary, our study identified the interaction between miR-512-3p and circ_0020123 or CORO1C for the first time. Circ_0020123 knockdown suppressed the malignant potential of NSCLC cells via miR-512-3p-dependent regulation of CORO1C, which brings new light to NSCLC therapy.

CONFLICT OF INTEREST

The authors declare that they have no conflicts of interest.

ORCID

Meiling Yang  <https://orcid.org/0000-0002-9690-5458>

REFERENCES

- Gong JL, Qiu W, Zeng Q, Liu X, Sun X, Li H, et al. Lack of short-chain fatty acids and overgrowth of opportunistic pathogens define

- dysbiosis of neuromyelitis optica spectrum disorders: a Chinese pilot study. *Mult Scler J*. 2019;25:1316–25.
2. Jonna S, Subramaniam DS. Molecular diagnostics and targeted therapies in non-small cell lung cancer (NSCLC): an update. *Discov Med*. 2019;27:167–70.
 3. Reungwetwattana T, Weroha SJ, Molina JR. Oncogenic pathways, molecularly targeted therapies, and highlighted clinical trials in non-small-cell lung cancer (NSCLC). *Clin Lung Cancer*. 2012;13:252–66.
 4. Chen LL, Yang L. Regulation of circRNA biogenesis. *RNA Biol*. 2015;12:381–8.
 5. Kristensen LS, Andersen MS, Stagsted LVW, Stagsted LV, Ebbesen KK, Hansen TB, et al. The biogenesis, biology and characterization of circular RNAs. *Nat Rev Genet*. 2019;20:675–91.
 6. Gao JL, Chen G, He HQ, Wang J. CircRNA as a new field in human disease research. *Zhongguo Zhong Yao Za Zhi*. 2018;43:457–62.
 7. Meng S, Zhou H, Feng Z, Xu Z, Tang Y, Li P, et al. CircRNA: functions and properties of a novel potential biomarker for cancer. *Mol Cancer*. 2017;16:94.
 8. Huang M, He YR, Liang LC, Huang Q, Zhu ZQ. Circular RNA hsa_circ_0000745 may serve as a diagnostic marker for gastric cancer. *World J Gastroenterol*. 2017;23:6330–8.
 9. Qu D, Yan B, Xin R, Ma T. A novel circular RNA hsa_circ_0020123 exerts oncogenic properties through suppression of miR-144 in non-small cell lung cancer. *Am J Cancer Res*. 2018;8:1387–402.
 10. Bi R, Wei W, Lu Y, Hu F, Yang X, Zhong Y, et al. High hsa_circ_0020123 expression indicates poor progression to non-small cell lung cancer by regulating the miR-495/HOXC9 axis. *Aging*. 2020;12:17343–52.
 11. Wan J, Hao L, Zheng X, Li Z. Circular RNA circ_0020123 promotes non-small cell lung cancer progression by acting as a ceRNA for miR-488-3p to regulate ADAM9 expression. *Biochem Biophys Res Commun*. 2019;515:303–9.
 12. Wang L, Zhao L, Wang Y. Circular RNA circ_0020123 promotes non-small cell lung cancer progression by sponging miR-590-5p to regulate THBS2. *Cancer Cell Int*. 2020;20:387.
 13. Lee YS, Dutta A. MicroRNAs in cancer. *Annu Rev Pathol*. 2009;4:199–227.
 14. Mishra S, Yadav T, Rani V. Exploring miRNA based approaches in cancer diagnostics and therapeutics. *Crit Rev Oncol Hematol*. 2016;98:12–23.
 15. Hansen TB, Jensen TI, Clausen BH, Bramsen JB, Finsen B, Damgaard CK, et al. Natural RNA circles function as efficient microRNA sponges. *Nature*. 2013;495:384–8.
 16. Zhu X, Gao G, Chu K, Yang X, Ren S, Li Y, et al. Inhibition of RAC1-GEF DOCK3 by miR-512-3p contributes to suppression of metastasis in non-small cell lung cancer. *Int J Biochem Cell Biol*. 2015;61:103–14.
 17. He L, Hannon GJ. MicroRNAs: small RNAs with a big role in gene regulation. *Nat Rev Genet*. 2004;5:522–31.
 18. Liao M, Peng L. MiR-206 may suppress non-small lung cancer metastasis by targeting CORO1C. *Cell Mol Biol Lett*. 2020;25:22.
 19. Livak KJ, Schmittgen TD. Analysis of relative gene expression data using real-time quantitative PCR and the 2^(-Delta Delta C [T]) method. *Methods*. 2001;25:402–8.
 20. Zhang HD, Jiang LH, Sun DW, Hou JC, Ji ZL. CircRNA: a novel type of biomarker for cancer. *Breast Cancer*. 2018;25:1–7.
 21. Kristensen LS, Hansen TB, Venø MT, Kjems J. Circular RNAs in cancer: opportunities and challenges in the field. *Oncogene*. 2018;37:555–65.
 22. Pavlides S, Tsigirgos A, Vera I, Vera I, Flomenberg N, Frank PG, et al. Loss of stromal caveolin-1 leads to oxidative stress, mimics hypoxia and drives inflammation in the tumor microenvironment, conferring the "reverse Warburg effect": a transcriptional informatics analysis with validation. *Cell Cycle*. 2010;9:2201–19.
 23. Ruocco N, Costantini S, Costantini M. Blue-print autophagy: potential for cancer treatment. *Mar Drugs*. 2016;14:138.
 24. Chang Y, Yan W, He X, Zhang L, Li C, Huang H, et al. miR-375 inhibits autophagy and reduces viability of hepatocellular carcinoma cells under hypoxic conditions. *Gastroenterology*. 2012;143:177–187. e178.
 25. Sun H, Chen Y, Fang YY, Cui TY, Qiao X, Jiang CY, et al. Circ_0000376 enhances the proliferation, metastasis, and chemoresistance of NSCLC cells via repressing miR-384. *Cancer Biomark*. 2020;29:463–73.
 26. Chen T, Yang Z, Liu C, Wang L, Yang J, Chen L, et al. Circ_0078767 suppresses non-small-cell lung cancer by protecting RASSF1A expression via sponging miR-330-3p. *Cell Prolif*. 2019;52:e12548.
 27. Wang K, Sun H, Sun T, Qu H, Xie Q, Lv H, et al. Long non-coding RNA AFAP1-AS1 promotes proliferation and invasion in prostate cancer via targeting miR-512-3p. *Gene*. 2020;726:144169.
 28. Dou D, Ren X, Han M, Xu X, Ge X, Gu Y, et al. CircUBE2D2 (hsa_circ_0005728) promotes cell proliferation, metastasis and chemoresistance in triple-negative breast cancer by regulating miR-512-3p/CDCA3 axis. *Cancer Cell Int*. 2020;20:454.
 29. Shi Z, Shen C, Yu C, Yang X, Shao J, Guo J, et al. Long non-coding RNA LINC00997 silencing inhibits the progression and metastasis of colorectal cancer by sponging miR-512-3p. *Bioengineered*. 2021;12:627–39.
 30. Zhang G, Chen HX, Yang SN, Zhao J. MAGI1-IT1 stimulates proliferation in non-small cell lung cancer by upregulating AKT1 as a ceRNA. *Eur Rev Med Pharmacol Sci*. 2020;24:691–8.
 31. Fabian MR, Sonenberg N, Filipowicz W. Regulation of mRNA translation and stability by microRNAs. *Annu Rev Biochem*. 2010;79:351–79.
 32. Roadcap DW, Clemen CS, Bear JE. The role of mammalian coronins in development and disease. *Subcell Biochem*. 2008;48:124–35.
 33. Wang J, Tsouko E, Jonsson P, Bergh J, Hartman J, Aydogdu E, et al. Mir-206 inhibits cell migration through direct targeting of the Actin-binding protein coronin 1C in triple-negative breast cancer. *Mol Oncol*. 2014;8:1690–702.
 34. Cheng X, Wang X, Wu Z, Tan S, Zhu T, Ding K. CORO1C expression is associated with poor survival rates in gastric cancer and promotes metastasis in vitro. *FEBS Open Bio*. 2019;9:1097–108.

SUPPORTING INFORMATION

Additional supporting information may be found in the online version of the article at the publisher's website.

How to cite this article: Zhang H, Huang T, Yuan S, Long Y, Tan S, Niu G, et al. Circ_0020123 plays an oncogenic role in non-small cell lung cancer depending on the regulation of miR-512-3p/ CORO1C. *Thorac Cancer*. 2022;13:1406–18. <https://doi.org/10.1111/1759-7714.14408>